Crack Growth Rate of R7T Steel under Uniaxial Loading

Rychlost růstu trhliny oceli R7T při jednoosém namáhání

Ing. Vratislav Mareš, Lukáš Horsák

VŠB – Technical University of Ostrava, Laboratory of Integration of Material Assembly and Design, Regional Materials Science and Technology Centre, 17. listopadu 15/2172, 708 33 Ostrava-Poruba, Czech Republic

Fatigue is a phenomenon affecting most structural components during their operational life. The fatigue process has a direct effect on the lifespan of components, so the study of this degradation process is extremely important. In cases where a component is loaded under its design yield strength, it is very difficult to detect a crack in the early stages and thereby to avoid catastrophic failure. This paper investigates fatigue crack initiation and the fatigue crack growth rate in ferritic-pearlitic steel. It is primarily the microstructure of the material that plays an important role in the initial stages of fatigue cracks. Fatigue cracks in areas close to the threshold stress intensity factor range K_{th} are strongly influenced by the microstructural characteristics of the material, such as grain size, interlamellar distance, etc., as well as by the mean value of the applied stress. In the case of this steel, the microstructure consists of lamellar pearlite and ferrite netting around grain boundaries, where a key role is played by the size of grains and pearlitic colonies, as well as by the interlamellar spacing. In the area subject to Paris' law, the resistance to fatigue crack propagation can be influenced just by controlling the microstructure. Paris' law gives the relations between the amplitude of the stress intensity factor and subcritical crack growth rate. It can be expressed using the Paris law equation.

***Key words**: fatigue, ferritic-pearlitic steel; R7T steel; crack growth rate; fatigue crack initiation*

Únava materiálu je fenomén postihující většinu konstrukčních celků a zařízení během jejich provozního života. Únavový proces má přímý vliv na dobu života konstrukčních částí. Proto je studium tohoto degradačního procesu nesmírně důležité. V případech, kdy je konstrukční část zatěžována pod navrženou mezí kluzu, je velmi obtížné odhalit trhlinu již v raných stádiích, a tím předejít fatálním kolapsům konstrukčních celků. V této práci je studována iniciace únavové trhliny a rychlost jejího šíření ve feriticko-perlitické oceli. Především mikrostruktura materiálu hraje významnou roli v počátcích iniciace únavových trhlin. Únavová trhlina při namáhání v oblastech blízkých prahové hodnotě faktoru intenzity napětí K_{th} je silně ovlivněna mikrostrukturálními charakteristikami materiálu (velikost zrna, mezilamelární vzdálenost), ale také střední hodnotou aplikovaného napětí. Materiál, který je použit v této práci je podeutektoidní feriticko-perlitická ocel R7T, která se běžně používá pro výrobu železničních kol. Protože konstrukce železničního kola je silně exponována na únavu a okolními podmínkami, je nanejvýš vhodné studovat právě tento uvedený materiál. V případě použité podeutektoidní oceli je mikrostruktura tvořena lamelárním perlitem a feritickým síťovím, kde hraje roli velikost zrna, perlitické kolonie a mezilamelární vzdálenost. Odpor proti šíření únavové trhliny v oblasti platnosti Parisova zákona může být ovlivněn právě mikrostrukturou. Parisův zákon, známý též jako Paris-Erdoganův zákon, dává do relace rozkmit faktoru intenzity napětí s podkritickým růstem trhliny.

***Klíčová slova**: únava materiálu; feriticko-perlitická ocel; ocel R7T; rychlost růstu trhliny; iniciace únavového poškození*

Many researchers studied fatigue behavior and fatigue crack growth. The results were primarily focused on in-situ testing of very small specimens. Most of the works are–focused on the effect of microstructure on fatigue initiation and observing changes in the microstructure of tested material, such as a slip bands [3, 4]. On the other hand, research regarding the effect of microstructure on fatigue crack growth behavior in the so-called Paris regime has rarely been reported [4]. Although only limited information is available on the detailed influence changing load amplitude on fatigue crack growth rate, some important works on fatigue crack growth behavior of two-phase steels have been reported [4 – 9].

The main objective is to focus on the influence of the applied stress amplitude to the fatigue crack growth rate of commonly used material for railway wheels. The aim of the presented paper is to analyze fatigue crack growth and the evolution of crack path of railway wheel steel R7T under fatigue loading with different amplitude. To this end, fatigue testing was performed on flat specimens, examining of crack at the macroscopic and microscopic levels to determine crack length and path were performed using confocal and electron microscopy.

In the presented study, fatigue crack growth rate tests were carried out on servo-hydraulic testing machine

Hutnické listy č. 5/2017, roč. LXX
ISSN 0018-8069

step by step. Between each step observations and measurements were conducted on the laser scanning confocal microscope and on the electron microscope.

Material

The material employed in this paper is hypoeutectoid ferritic-pearlitic steel R7T (Fig. 1), which is commonly used for the manufacture of railway wheels. This is because the structure of railway wheels is heavily exposed to the effects of fatigue and environmental conditions. The material is a highly appropriate subject for study. of hypoeutectoid ferrite-pearlite steel R7T, which is used in the production of railway wheels and which is defined in European Standard EN13262. The chemical composition of this steel was obtained by optical emission spectroscopy and is shown in Tab. 1, which does not differ from the commercial standard for this material.

Tab. 1 Chemical composition
Tab. 1 Chemické složení

Element	C	Mn	Si	P	S	Cr	Ni	Mo	Cu	Ti	Al
wt. %	0.385	0.824	0.496	0.007	0.003	0.24	0.074	0.010	0.01	0.001	0.022

The R7T steel was heat treated in the following way: austenitization at the temperature of 850 °C/water cooling and tempering at the temperature of 520 °C. The final microstructure resulting from the heat treatment of the commercially produced wheel, in general terms, was a mixture of lamellar pearlite with a small quantity of ferrite.

From the metallographic point of view, it is fine-grained ferritic - pearlitic structure or lamellar pearlite with the ferritic networking. The pearlite as a two-phase material consisting of hard and brittle lamellar cementite in ferritic matrix significantly affects the life of the material exposed by time-varying stress component.

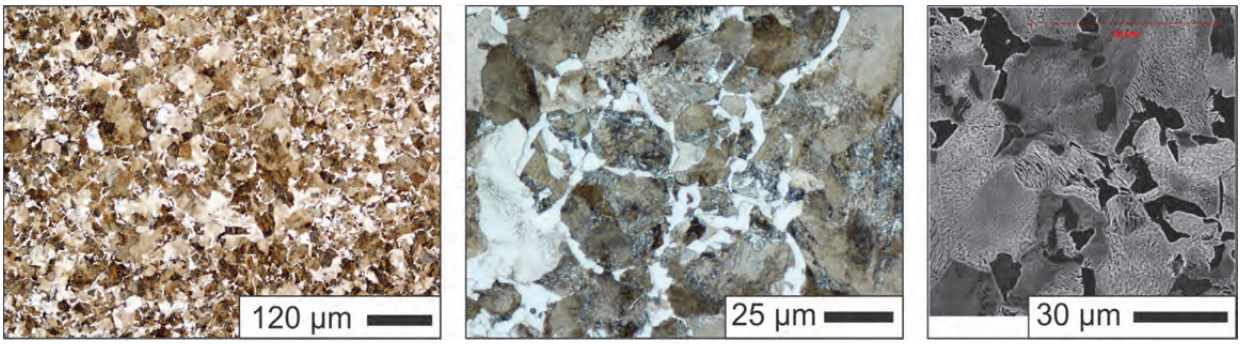

Fig. 1 Microstructure of R7T steel, right-low magnification, center-high magnification (optical microscopy), right - SEM photography, (etched in 3% Nital)
Obr. 1 Mikrostruktura oceli R7T, vlevo malé zvětšení, uprostřed velké zvětšení, vpravo fotografie SEM (leptání v 3% roztoku Nitalu)

Regarding the metallographic analysis, the structure of the material was formed by the lamellar pearlite bounded by ferritic networking. The microstructures in Fig. 1 were obtained by standard metallographic procedure, by grinding - polishing - etching in 3% Nital solution, and the photographs were obtained by using optical and electron microscope. Tab. 2 shows basic microstructural properties of the material.

Tab. 2 Microstructural properties
Tab. 2 Mikrostrukturní vlastnosti

Grain size	G10/11 µm
Average interlamellar distance	0.53 µm
Hardness *HV10*	228

The mechanical, or tensile properties of R7T are shown below in Tab. 3. Knowledge of this mechanical properties is very beneficial for setting fatigue test parameters.

Tab. 3 Mechanical properties
Tab. 3 Mechanické vlastnosti

Yield strength R_{p02}	515 MPa
Ultimate strength R_m	837 MPa
Elongation A_{10}	14.1 %
Fracture toughness K_{IC}	87.96 MPa·m$^{1/2}$

Specimens and testing procedure

All specimens were tested on fatigue biaxial servohydraulic machine INSTRON 8802. The soft control mode was chosen, typical for high-cycle fatigue. It means that the machine was driven only by force. The tests were conducted using a sinusoidal form of loading with a stress ratio of 0.1 and a frequency of 5 Hz. The shape of varying force corresponded with sinus function.

Single edge cracked plates of tension type specimens with a width of 5 mm and a thickness of 1.5 mm were used for fatigue crack growth tests (Fig. 2). A notch with a width of 0.25 mm and a depth of 0.5 mm was formed by electric discharge machining (EDM) at the edge of the specimen as a starter for fatigue crack growth prior to the fatigue crack growth test.

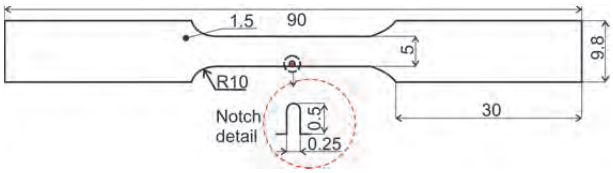

Fig. 2 Specimen geometry for fatigue crack growth test (dimensions in mm)
Obr. 2 Geometrie vzorku pro zkoušky šíření únavových trhlin (rozměry v mm)

The specimen surface was prepared for observation of crack growth by grinding and polishing with the use of 1 µm diamond solution. The whole specimen was etched in 3% Nital solution but the notch area was masked against etching. The masked area around EDM notch was a circle with a diameter of approx. 0.5 mm. Masking was performed because etched surface could have influenced crack growth in initiation stages, because the etched surface locally reinforced. A strain gauge was placed in the center of the selected specimen for deformation monitoring.

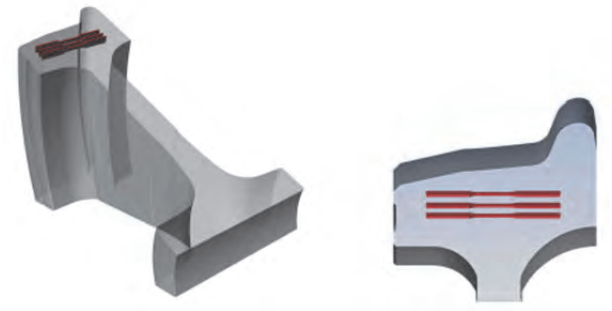

Fig. 3 Specimen location in railway wheel
Obr. 3 Odběr vzorku ze železničního kola

In Fig. 3 location of the specimen in the railway wheel is visible. The main position is in the center of the wreath under the running surface of the railway wheel.

The stress intensity factor K, for the present specimen was calculated according to the following eq. 1 and 2 [2, 5]:

$$K = \sigma\sqrt{\pi a} \cdot F_1(\alpha), \alpha = \frac{a}{W} \quad (1)$$

$$F_1(\alpha) = 1.12 - 0.231\alpha + 10.55\alpha^2 - 21.72\alpha^3 + 30.39\alpha^4 \quad (2)$$

where σ is the stress, a is the crack length, W is the width of the gauge part of the specimen and F_1 is a geometrical correction factor [2, 3, 4].

Tab. 4 shows used stress levels, which were applied during testing of specimens. This table primarily shows the stress amplitude, other values are for information with respect of cycle asymmetry coefficient R = 0.1.

Testing was realized step by step. That means that after numbers of cycles the test was stopped and the specimen was measured in the microscope. The specimen measurement was was then followed by numbers of test cycles.

Tab. 4 Applied stress levels
Tab. 4 Aplikované úrovně napětí

Load level	Stress amplitude σ_a	Mean stress σ_s	Minimal stress σ_{min}	Maximal stress σ_{max}
	(MPa)			
I	225	275	50	500
II	220.5	269.5	49	490
III	207	253	46	460
IV	202.5	247.5	45	450
V	135	165	30	300
VI	126	154	28	280

Results and discussion

During testing many measurements were conducted and many photos were taken. All results are presented in graphical and tabular form. Fig 4 shows the fatigue crack path and crack growth rate for the specimen No. 4.

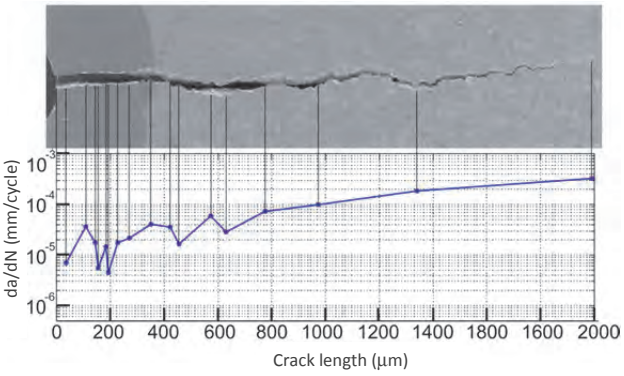

Fig. 4 Relation between the crack growth rate and crack length in combination with visual documentation of total length of crack before fracture
Obr. 4 Závislost mezi délkou a rychlostí růstu trhliny s vizuální dokumentací celkové délky trhliny těsně před porušením

Hutnické listy č. 5/2017, roč. LXX
ISSN 0018-8069

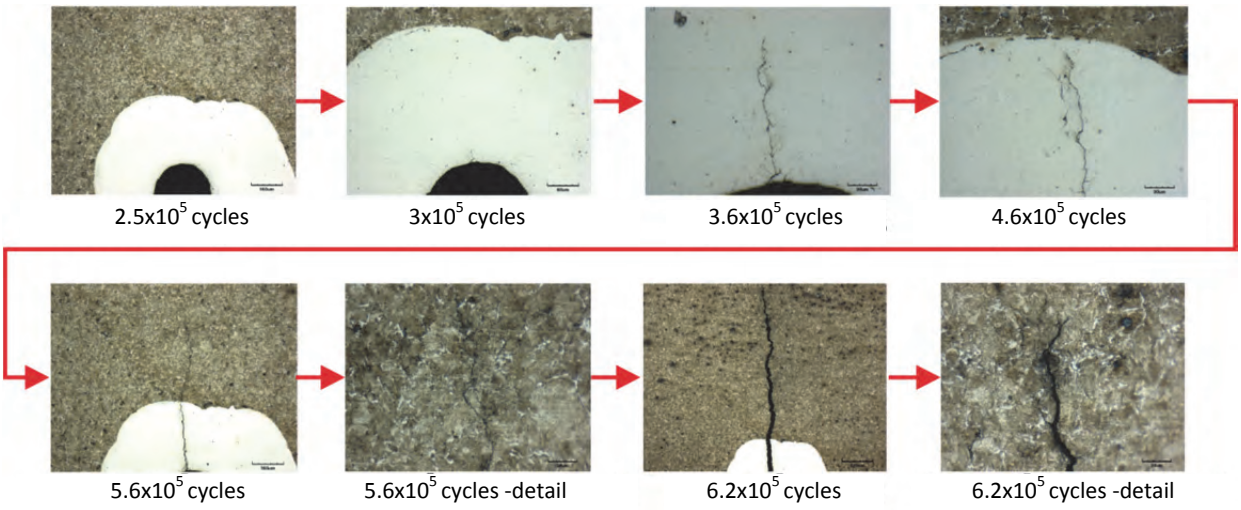

Fig. 5 Visualized crack path step by step
Obr. 5 Vizualizovaný růst trhliny

Fig. 5 shows the detailed crack propagation step by step from the initiation stage to the final crack length. The masked area around the EDM notch is well visible.

Calculations were conducted according to Paris-Erdogan law [2, 5]:

$$\frac{da}{dN} = C \cdot \Delta K^m \tag{3}$$

Tab. 5 shows all acquired and measured results. Material constants of Paris law, i.e. C and m were obtained by nonlinear fit [6] by least squares method using the MATLAB software.

Tab. 5 Final results for all specimens
Tab. 5 Finální výsledky pro všechny vzorky

Specimen	Load level	Cycles to failure *Nf*	ΔK (MPa·m$^{1/2}$)	*C*	*m*
1	I	5,454	33.47	8.84e-10	3.67
2	II	7,100	53.26	2.72e-9	3.12
3	III	7,882	23.74	2.72e-8	2.96
4	IV	46,276	74.35	2.72e-8	2.41
5	V	49,204	76.99	2.46e-8	2.41
6	VI	62,765	62.58	2.72e-8	2.27
7	VI	72,238	97.59	4.60e-8	2.25

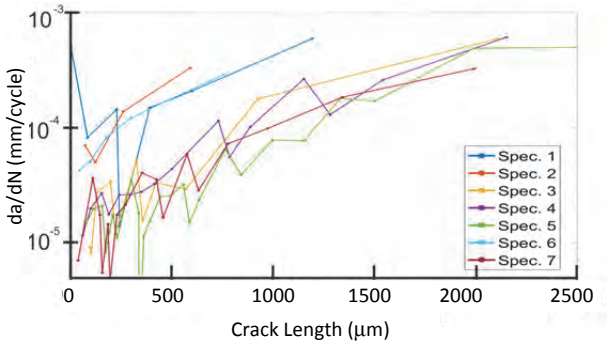

Fig. 6 Comparison of the average crack growth rates vs. crack length
Obr. 6 Porovnání průměrné rychlosti růstu a délky trhliny

Comparison between crack growth rates vs crack length is presented in Fig. 6. The differences between specimens and their loading state are clearly visible. Generally, curves have an increasing trend in relation to the applied load. The observed declines (piles down) are caused by interruptions for measurement during testing, or by fastening of specimens [6, 7].

Fig. 7 shows crack paths in the microstructure of the R7T steel. Red arrows basically highlight crack path. Left photography demonstrates the crack growth along the grain boundaries – for specimens loaded with low-stress amplitudes. The right photograph shows the crack growth across the grain due to higher stress amplitudes and local overloading. This is caused by the brittleness of cementite lamellae, which not carry over greater load [8, 9].

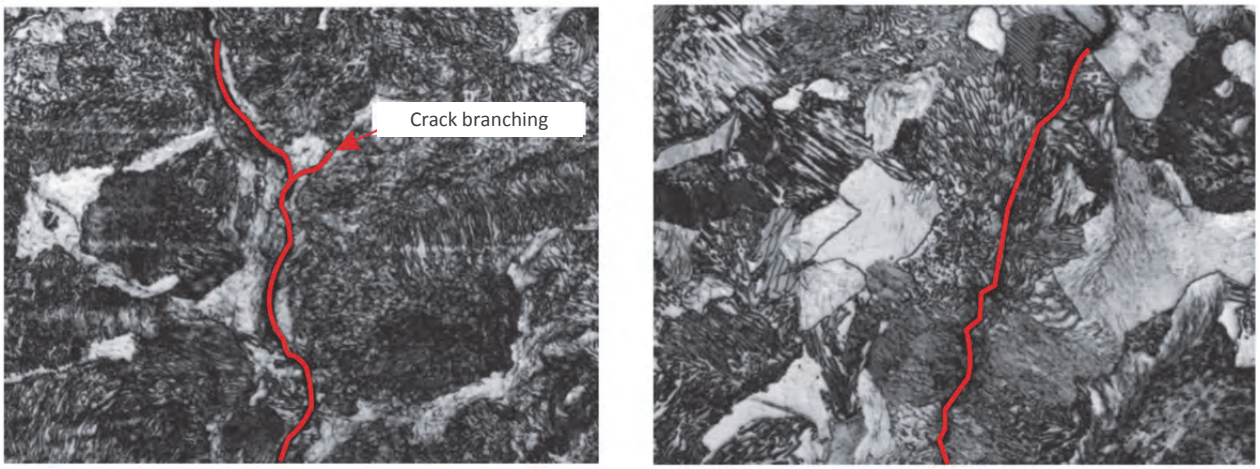

Fig. 7 Two cases of crack paths, left-along the grain, right-across the grain
Obr. 7 Dva případy růstu trhliny vlevo – podél hranice zrna, vpravo - přes zrno

Conclusions

During experimental testing of notched specimens of steel, R7T a large amount of images and numerical data was obtained that were processed and gradually explained. From results relationships were compiled of the obtained parameters and crack growth rate. Crack under cyclic stress growth along the grain boundaries across ferrite network – were simply slip system. Sometimes, crack growth occurred across the grain with pearlite lamellae - probably due to effect of multi-axis stress state. The above-obtained data enabled an optimized design and predictions of fatigue behavior.

A lot of tests were performed in order to verify the crack growth rate of R7T steel. Fatigue cracks initiation stages was studied. Micromechanism of initiation, which would increase fatigue strength, was investigated. Samples without a notch were tested. Application of influence of multiaxial stress state was studied. Summary of the experimentally obtained data led to the preparation of material model for the simulation of fatigue crack growth in the steel R7T.

The presented results will help to improve or clarify the effect of fatigue damage in the real structure of the railway wheels. Despite large of amount of acquired a lot of issues has still remained unresolved, both in the existing and new materials. Therefore, it is important to continue to carry out measurement and experimental study of fatigue damage mainly in the initiation stages. [7-9]

Acknowledgement

*This paper was created within the **Project No. LO1203 "Regional Materials Science and Technology Centre - Feasibility Program**" funded by Ministry of Education, Youth and Sports of the Czech Republic.*

Literature

[1] BEDEN, S. M., ABDULLAH, S., ARIFFIN, A. K. Review of Fatigue Crack Propagation Models for Metallic Components. *European Journal of Scientific Research*, (2009) 3, 364–397.

[2] ELLYIN, F. *Fatigue Damage, Crack Growth and Life Prediction*, Chapman & Hall, 1997, 468 pp.

[3] KHEN, R., ALTUS, E. Micro-macro Relations for Fatigue Crack Growth. *Mechanics of Materials*, (1995) 2(3), 89–101, ISSN 0167-6636.

[4] KORDA, AA., MIYASHITA, Y., MUTOH, Y., SADASUE, T. Fatigue Crack Growth Behavior in Ferritic-pearlitic Steels with Networked and Distributed Pearlite Structures. *International Journal of Fatigue*, 29 (2007) 6, 1140–1148, ISSN 0142-1123.

[5] LAWSON, L., CHEN, EY, MESHII, M. Near-threshold Fatigue: a review. *International Journal of Fatigue*, (NOV 1999) 21, Supplement S, S15–S34, ISSN 0142-1123.

[6] LIU, Y., STRATMAN, B., MAHADEVAN, S. Fatigue Crack Initiation Llife Prediction of Railroad Wheels. *International Journal of Fatigue*, 28 (2006) 7, 747–756, ISSN 0142-1123.

[7] MUGHRABI, H. Microstructural Fatigue Mechanisms: Cyclic Slip Irreversibility, Crack Initiation, Non-linear Elastic Damage Analysis. *International Journal of Fatigue*, 57 (2013) SI, 2–8. ISSN 0142-1123.

[8] LADOS, D. A., APELIAN, D. Relationships between Microstructure and Fatigue Crack Propagation Paths in Al-Si-Mg Cast Alloys. *Engineering Fracture Mechanics*, 75 (2008) 3-4, 821–832. ISSN 0013-7944.

[9] TORIBIO, J., GONZALES, B., MATOS, J.C. Fatigue and Fracture Paths in Cold Drawn Pearlitic Steel. *Engineering Fracture Mechanics*, 77 (2010) 11, 2024–2032. ISSN 0013-7944.